Ultramicroscopy 113 (2012) 77–82

Contents lists available at SciVerse ScienceDirect

Ultramicroscopy

journal homepage: www.elsevier.com/locate/ultramic

On the dose-rate threshold of beam damage in TEM

Nan Jiang *, John C.H. Spence

Department of Physics, Arizona State University, Tempe AZ 85287-1504, USA

ARTICLE INFO

Article history:
Received 6 June 2011
Received in revised form
18 November 2011
Accepted 23 November 2011
Available online 8 December 2011

Keywords:
Beam damage
Dose rate threshold
(S)TEM
EELS

ABSTRACT

Electron beam damage in a CaF_2–Al_2O_3–SiO_2 glass is investigated using time-dependent Ca L_{23} and O K-edge electron energy-loss spectroscopy. It appears that there is a threshold dose rate, below which the damage involving the formation of O defects may not be detected, at any total dose. This suggests that the threshold phenomenon of dose rate may result from the competition of damage and recovery processes. The accumulation of damage can only occur when the damage rate is higher than the recovery rate. For surface sputtering process in TEM, the recovery rate is negligible. Therefore, there is no threshold dose rate for surface sputtering.

1. Introduction

Radiation damage remains an important obstacle to extend applications of (scanning) transmission electron microscopy (TEM/STEM). Aberration correction allows the STEM objective aperture (condenser aperture in TEM nanodiffraction mode) to be enlarged so that the electron probe on the specimen may have a very high current density, e.g. $>10^6$ A/cm^2 [1]. This value is about 10^4–10^5 times larger than the current density used in forming conventional HREM images, and about 10^6–10^7 larger than that used for bright-field diffraction contrast imaging. Can materials survive under these conditions?

The various phenomena associated with electron-beam damage in TEM/STEM have been extensively studied in recent decades [for a review, see [2,3]]. In brief, electron-beam damage in specimens is mainly caused by the following three mechanisms. One is due to knock-on interaction through elastic scattering, in which the incident electrons transfer kinetic energy and momentum to atoms. If the kinetic energy acquired by an atom is higher than its displacement threshold energy (E_d) or surface binding energy (E_s), the atom may be displaced from its site to an interstitial or vacancy, forming a Frenkel pair in the bulk, or sputtered away from surfaces into vacuum. In TEM/STEM, the surface sputtering process usually dominates the former one, because E_s is usually much smaller than E_d. Next is radiolysis, which is due to ionization process through inelastic scattering. Some of the criteria required for radiolysis in TEM/STEM are: the excitation needs to be localized for a time long enough for the atom to respond mechanically, and the energy acquired by the excited atom must be convertible into momentum, resulting in atomic displacements [2]. Therefore, beam damage due to radiolysis process may occur in electronically insulating materials. It is suggested that radiolysis is responsible for the formation of F- and H-centers in alkali halides and for amorphization of crystalline SiO_2 and silicates [4,5]. The third important mechanism is electrostatic charging of materials induced by the incident electron beam. Unlike SEM, charging in TEM/STEM is mainly caused by the ejection of secondary and Auger electrons into vacuum [6]. At high current density, the charge balance cannot be restored quickly enough by the environment, such as a Cu specimen supporter, for electronically insulating materials, and therefore a positive surface potential develops in the illuminated area. According to Cazaux [6], the estimated potential can be as high as 76 eV for a typical STEM probe with a diameter of 1 nm and current of 0.4 nA (i.e. an electron current density $\sim$0.4 nA/nm^2), thus the maximum radial component of electric field at the edge of probe can be higher than 10^{10} V/m. This value is much larger than the breakdown voltages of most dielectric materials. Therefore, the positive potential induced by the incident electron may cause a lateral migration of cations and anions, drawing anions into the irradiated area and expelling cations [7,8]. As for radiolysis, electrostatic charging only occurs in insulating materials. In many cases, in fact, the last two mechanisms cannot be distinguished, especially in the case of a highly intense and focused electron probe.

To avoid electron-beam damage, or to utilize the electron probe for direct-write lithography in TEM/STEM, it is crucially important to understand the damage thresholds of various

* Corresponding author. Tel.: +1 480 7277169.
E-mail address: nan.jiang@asu.edu (N. Jiang).

0304-3991/$ - see front matter © 2011 Elsevier B.V. All rights reserved.
doi:10.1016/j.ultramic.2011.11.016

mechanisms. The energy threshold for knock-on damage is well understood [9,10]. It can be calculated reasonably accurately as long as E_d or E_s is known [11]. The energy threshold effect in ionization (radiolysis) damage has also been studied. Although there is still debate on whether the damage is dominated by the ionizations of inner shells [12–14] (which dump large amounts of energy, but less frequently) or valence exciton excitations [4] (which dump smaller amounts but more frequently), the energy threshold in radiolysis damage is generally unimportant since the kinetic energy of incident electrons in TEM/STEM (e.g. > 100 keV) is much higher than these thresholds.

Radiation damage is thought to depend on the energy absorbed by the target and its mass. The measure of the amount of radiation, the Gray, is thus defined as absorption of one joule of ionizing radiation by one kilogram of matter (1 Gy = 1 J/kg). In TEM/STEM, however, almost all the incident electrons pass through thin specimen. (Only a negligible portion of the electrons can be scattered laterally, and eventually absorbed by specimen after multiple scattering.) The energy deposited in specimens through inelastic scattering is only a small portion of total energy carried by the incident beam. Therefore, it is more convenient to use the number of incident electrons during an exposure (the fluence in C/cm^2 or e/nm^2), as the "electron dose", to represent the strength of irradiation in TEM/STEM. In the literature, this "dose" is defined as the product of electron current density (dose rate) and illumination (or exposure) time, and we will use this definition of dose in this paper. Generally, it has been considered that there is a "dose threshold", also known as the "critical dose" [15] or "characteristic dose" [16], for each beam-sensitive material, below which beam damage is negligible. The well-known low-dose technique commonly used for biological materials is based on this idea [17]. For a given total dose there are two ways to achieve a low-dose condition in TEM/STEM: either by lowering the electron current density (dose rate) or by shortening the exposure time. The former is widely used in the low-dose technique, but the disadvantage is its low signal-to-noise ratio (SNR) and poor resolution. The latter may increase the SNR, but the very short acquisition time may induce artifacts due to the finite detector response time [18]. Differences in image quality for the same dose but different exposure times (dose rate effects) are known as "reciprocity failure".

Although electron-beam damage has usually been measured using total dose in the electron microscopy literature [19], dose rate effects have also been noticed in a few cases [5,20]. A threshold for dose rate was observed in nanofabrication and hole-drilling studies on oxides and fluorides, which occur only above some threshold current density [21–23]. Here we report a threshold phenomenon for electron current density (dose rate) observed during electron-beam damage in a silicate glass. It was discovered that electron-beam induced damage in this CaF_2–Al_2O_3–SiO_2 glass was dependent on the beam current density (dose rate). Damage could not be detected if the current density (dose rate) was lower than the threshold value, for any total dose. The basis of this threshold dose rate effect is also discussed.

2. Experimental

The specimen used in this study was a CaF_2–Al_2O_3–SiO_2 glass. The method for the glass synthesis and TEM specimen preparation can be found elsewhere [24]. The experiments were carried out using a field-emission JEOL 2010F operating at 200 keV in TEM mode. The beam current density at the specimen was obtained approximately from the read-out of current density on the viewing screen, without specimen. The radiation damage in the specimen was monitored by the change in the O K- and Ca L_{23}-edge peaks in the electron energy-loss spectra (EELS). The EELS spectra were recorded by a Gatan Enfina electron spectrometer. The energy resolution was about1.0 eV measured by the full width at the half maximum (FWHM) of the zero-loss peak.

3. Calculation

The calculations of the density of states (DOS) and O K-edge EELS were carried out using the computer Code FEFF [25], which is based on a full-multiple scattering method. The method takes into account multiple scatterings of the excited core electron by the surrounding atoms, and the scattering is calculated by including a large number of atoms within a cluster. Self-consistent muffin-tin (MT) potentials were used in the calculations. The calculations were carried out using a structure model, which was

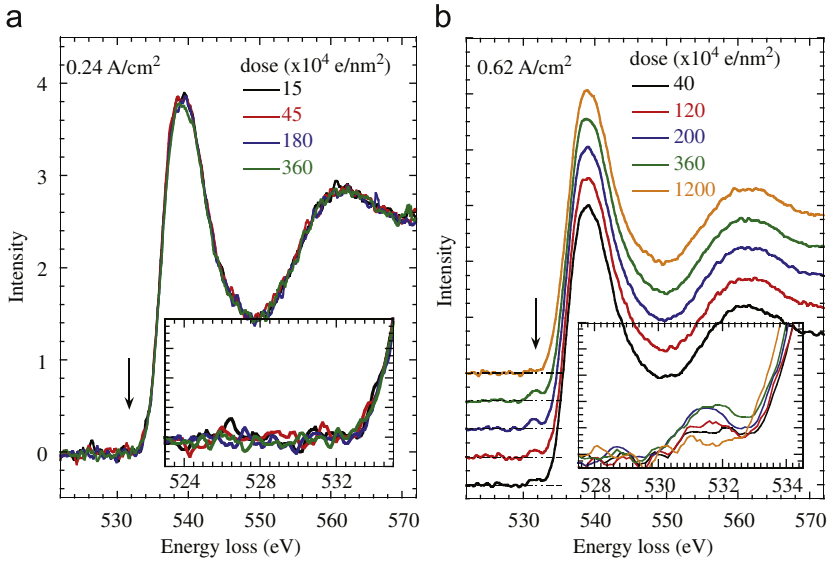

Fig. 1. Time series of O K-edge EELS spectra recorded at electron current density (dose rate) of (a) 0.24 A/cm^2 and (b) 0.62 A/cm^2, respectively. The insets are enlarged spectra for the onset energy region.

modified from mineral Melilite structure [26]. The cluster size was in the range 0.7–0.8 nm in radius.

4. Results and discussion

Fig. 1 compares two sets of O K-edge EELS spectra acquired under different electron current densities. Both sets of data were started in fresh regions immediately after exposure to the electron beam. Except for the beam current density, all other experimental parameters were the same, such as beam voltage (200 keV), acquisition areas (1 μm in diameter confined by the aperture of select area diffraction (SAD)), average thickness (according to the plural scattering intensity in the O K-edge EELS), collection aperture of EELS, acquisition time for each spectrum, magnification of image, and camera length of diffraction. At an electron current density of 0.24 A/cm^2, the O K-edge fine structure does not show measurable changes in time, especially at the onset region between 530 and 535 eV. By contrast, at an electron current density of 0.62 A/cm^2, the O K-edge shows significant changes at the onset region: initially a small bump between 530 and 533 eV increases and gradually disappears again. Evidently, this small pre-edge bump is induced by electron beam irradiation, and therefore is caused by the beam damage.

Fig. 2 plots the integrated intensities within an energy window (530–533 eV) containing the pre-edge bump, which are normalized to the corresponding integrated intensities of the O K-edge (530–550 eV). If the electron current density is less than 0.30 A/cm^2, as shown in Fig. 2a, the data are scattered between ± 0.003. This scattering may be due to the low SNR of raw data due to the low electron current density. The mean of these scattered data is about zero (-0.0002), and the standard deviation is 0.002. Therefore, the intensity of the pre-edge bump can be considered to be zero. This is consistent with the observations of spectra, in which no small bump can be unambiguously recognized at the onset region of O K-edge EELS.

Doubling the electron current density can significantly increase the SNR of the spectrum. As shown in Fig. 2b, the normalized intensity of the beam-induced pre-edge bump shows significant time dependence at a current density of 0.62 A/cm^2. The small bump rises rapidly within the first 40–50 s of irradiation, remains at about the same intensity ($\sim$0.006) for about 200 s after 50 s, and then quickly drops to an invisible level.

In Fig. 2, the accumulating dose (total numbers of electrons passing through the specimen per nm^2) for each data is also given. Interestingly, at the lower electron current density, the O K-edge does not show the pre-edge bump even through the accumulated electron dose is over 10^7 e/nm^2. By contrast, at the higher beam current density, the pre-edge bump occurred even though the accumulated dose is less than 10^6 e/nm^2. As compared in Fig. 3, in which two spectra were recorded at the same electron dose but at different dose rates, the pre-edge bump only can be observed at the higher dose rate. This evidence clearly indicates that the electron current density (dose rate) is more important than the dose to the beam damage, which results in the pre-edge bump in the O K-edge EELS. Therefore, if there is a threshold for the corresponding damage, it should be the threshold dose rate rather than the threshold dose.

Similar measurements were also carried out at different electron current densities. Summarizing all the data, the pre-edge bump in the O K-edge can be always observed whenever the current density is greater than 0.6 A/cm^2, while no change can be seen if the current density is less than 0.3 A/cm^2. In between, the data are not consistent: the pre-edge bump can be seen in some measurements but not in others. Therefore, we suggest that there

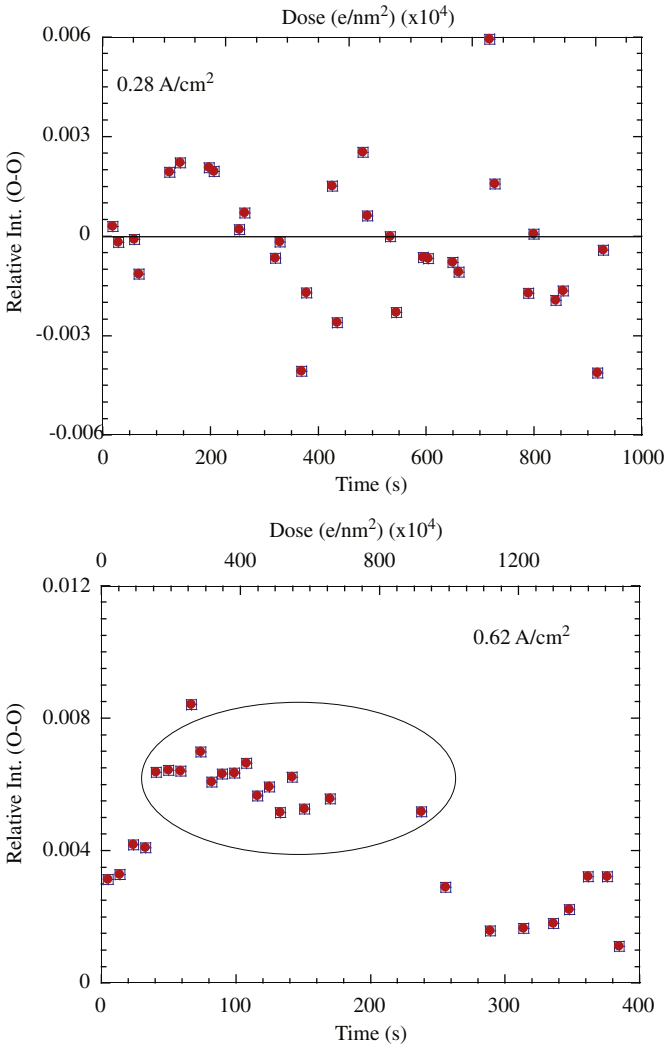

Fig. 2. Ratio of integrated intensities at onset region to total O K-edge.

is a threshold dose rate, above which the sample can be damaged to create the pre-edge bump in the O K-edge EELS. At 200 keV, this threshold dose rate should be in between 0.3 and 0.6 A/cm^2 for this particular glass.

The beam damage induced pre-edge peak in the O K-edge has been widely observed in various silicate minerals and glasses [27], as well as in non-silicate oxides, such as $MgAl_2O_4$ crystal [28] and $CaAl_2O_4$ glass [29]. The origin of the pre-edge peak in the O K-edge is associated with beam-induced defects, such as O–O peroxyl bonds, O_2 molecules, and/or O_2 clusters. These O defects can be induced by radiolysis process, as proposed by Hobbs and his colleagues [5]. The strong O–O interaction can produce an unoccupied antibonding π^* peak [30], which is located before the onset energy of O K-edge EELS, resulting in the pre-edge peak in O K-edge.

Furthermore, we suggest that the pre-edge peak in the O K-edge EELS is also induced by the formation of O dangling bonds (or unpaired O), which are caused by the removal of cations (Ca^{2+} in this case) from their sites by strong electrostatic field due to the charging effect. The formation of unpaired O is schematically illustrated in Fig. 4, using a structure model of modified mineral Melilite structure [26]. Fig. 5 compares the projected DOS on the oxygen (indicated by arrows in Fig. 4) before and after removal of a nearby Ca ion. The atom potentials used in both structural models were all constructed from the self-consistent calculations

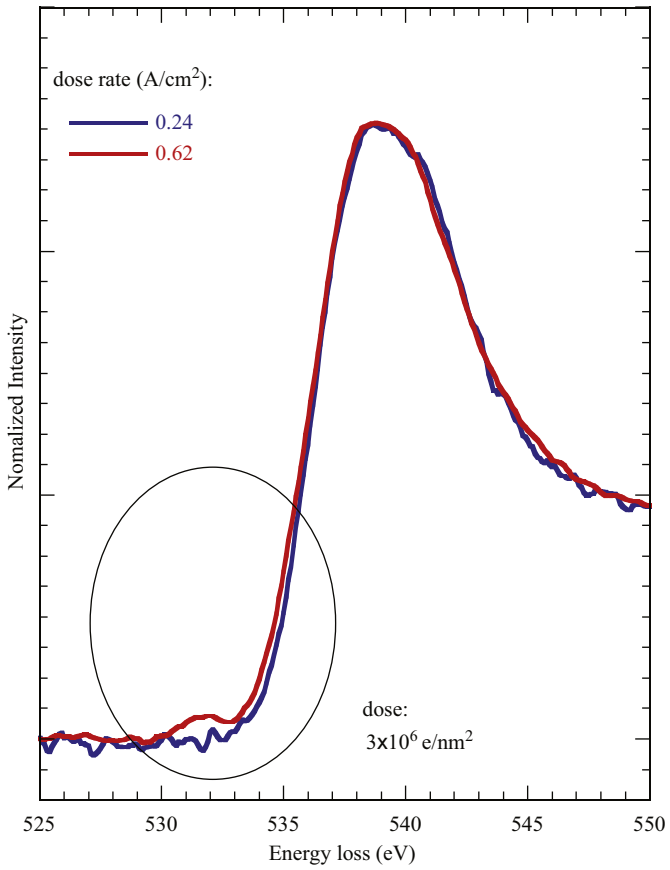

Fig. 3. Comparison of O K-edge EELS at two different dose rates but the same total dose. These two spectra are reproduced from Fig. 1.

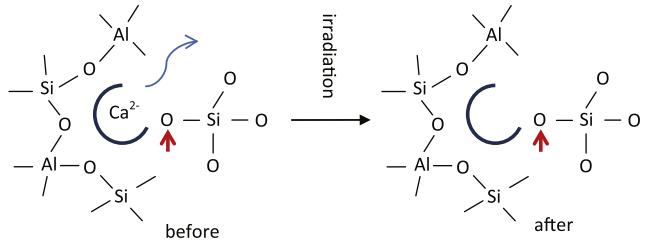

Fig. 4. Schematic drawings showing a model of the ejection of a Ca ion during beam damage process.

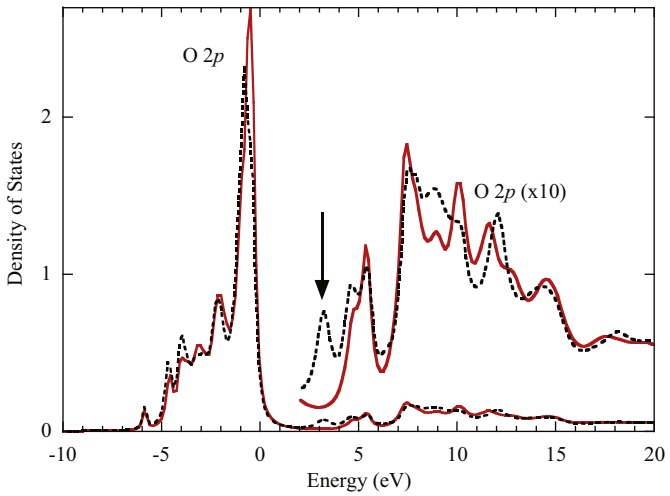

Fig. 5. Comparison of calculated partial DOS projected on O before and after removing a nearby Ca atom.

in the original structure. Therefore, the calculated Fermi energies do not change in these two cases. As shown in Fig. 5, it is clearly shown that the removal of the nearby Ca can introduce a small peak in O 2p-DOS before the edge of O 2p unoccupied states. This peak is also responsible for the pre-edge peak observed in the O K-edge induced by electron irradiation.

The unpaired O may not be stable. The vacancy left by the displaced Ca could be filled by a nearby O, forming O–O peroxyl bond or even O_2 molecule. This process could result in the damage to be "permanent", because these O may not return to their original sites. Instead, they could diffuse out of the sample, or even form O_2 bubbles [31]. If this process continues, the pre-edge peak at the O K-edge will further increase or remain until the O_2 molecules diffuse out of the sample or the O_2 gas bubbles burst. On the other hand, the unpaired O could also attract the displaced Ca back or other Ca ion to fill the vacancy, annealing the defect created by irradiation damage. This process leads the specimen to recover from the damage. Therefore, we consider the former as the damaging process and the latter as the recovering process. The unpaired O is then a transient state.

Strictly speaking, beam damage in specimen should include any change to the specimen. In practice, however, beam damage can only be detected when the accumulation of damage reaches a threshold, due to the limitation of instrument sensitivity. This amount can be considered as a critical point, which determines whether the acquired information is still representative of the original object. The instrument-determined critical point may be coincident with the previously mentioned critical dose or characteristic dose [15,16], if the accumulation of damage is proportional to the electron dose. Therefore, the more advanced the TEM/STEM, the more difficult it is to obtain damage-free information. This is only due to the destructive nature of electron beam.

Some damage, but not all, can be "self-cured" by the specimen. As discussed in the above case, although the displacement of Ca leaves unpaired O, there is a possibility that the unpaired O may attract this displaced Ca back or another Ca ion from nearby to anneal the damage. Therefore, there are always two rates governing the damage process: the rate of damage and the rate of recovery. Damage accumulation can only occur if the former dominates the latter. Although the explicit evaluation of these two rates is difficult, it is reasonable to consider that the damage rate is proportional to the electron current density or dose rate. In other words, the beam damage can also depend on dose rate. Therefore, it is likely that both a threshold dose and a threshold dose rate may exist. The former is determined by the sensitivity of instrument, but the latter is an intrinsic property of the specimen.

Interpretation of the dose rate threshold phenomena is not as simple as the energy threshold. It requires an understanding of the detailed dynamics of the damage and recovery processes. Perhaps one of the crucial factors one needs to consider is the difference between the time for an electronic excitation and the time for atomic displacement. The former is of order of *fs* while the latter is of order of *ps* [2]. For example, at time t_1, the first beam electron enters the specimen and creates an electronic excitation within time of T_1. This excited state has a long enough life time, T_2, to allow an atom to become displaced. Here, $T_2 \gg T_1$. Perhaps it will take about the same order of time for the displaced atom to return to its original site. Therefore, the specimen may be recovered from the damage induced by the first incident electron at time t_2 ($t_2 \geq T_2$). If the incident electrons enter the specimen with time interval of t_3, which is determined by beam current density (or dose rate), and $t_3 \gg t_2$, the chance is that the second

electron entering the specimen may not see the previous electron induced atom displacement (damage). In other words, if the incident electron intensity is very low, the specimen may have long enough time to recover from the damage induced by the previous electrons before the consecutive electrons come in. Therefore, the beam damage cannot be detected no matter how many accumulated electron dose is. By contrast, if electron current density is so high that $t_3 \ll t_2$, the beam damage induced by the previous electrons can be easily detected by consecutive electrons. It should be pointed out that the difference between t_2 and t_3 depends not only on the incident electron intensity, but also on how easy the specimen can be restored, i.e. the displaced atoms return to the original sites. If the specimen has defects, such as dislocations or grain boundaries, the displaced atoms may have tendency to rest in these low energy sites, thus the probability to return to the original sites is very small. In this case, $t_3 \ll t_2$ no matter how weak the beam intensity is, because $t_2 \to \infty$.

For a 200 kV accelerating voltage, the velocity of incident electron is about 0.7 c (c: the speed of light). Assuming that specimen thickness is 100 nm, the time for an incident electron pass through the specimen is about 1/2 fs, which is about the same magnitude of time for electronic excitation process. Assuming that the distance for atom displacement is about a nanometer, it is convenient and appropriate to use nm^2 as unit area and e/nm^2 s to represent electron current density (or dose rate). For the typical electron current density used in this study, for example, $0.6\ A/cm^2 = 3.75 \times 10^4\ e/nm^2\ s$. Therefore, the interval (t_3) between two consecutive electrons within the area of 1 nm^2 is about 30 μs. In other words, the specimen may have 30 μs to recover from the damage produced by the previous electron. If the displacement or diffusion distance can reach e.g. 10 nm, the unit area is then $10^2\ nm^2$. In this case, $t_3 = 0.3$ μs. This is still a quite long time for specimen to recover, if it can. By contrast, for the aberration corrected STEM probe ($10^6\ A/nm^2$), $t_3 = 1.6 \times 10^{-25}$ s. This means $t_3 \ll t_1 \ll t_2$. Therefore, the specimen may not have chance to recover from any damage if there is any.

The above estimate is a crude approximation. The detailed dynamics for damage and recovery processes are very complicated. Some other parameters which could also be important include thermal conductivity, electric conductivity, density of defects, and activation energies for defects. All these factors may directly affect both the damage and recover rates, and thus alter the above estimated durations of processes. Another important factor in beam damage is the cross section of inelastic scattering, which is the probability of ionization event. Adding cross section to the estimation can lower the damage rate, but does not change the duration of either process. Nevertheless, further comprehensive investigation is needed to quantify the theory.

One extreme case is surface sputtering, in which the sink for displaced atoms is infinitely large. Therefore, the recovery rate can be considered as zero. Then, as long as the beam energy exceeds E_s for a specific element, the sputtering of this species will occur. Fig. 6 shows the integrated intensities of the Ca L_3 and O K-edge EELS in the specimen. Both series of spectra were taken from the same area, in diffraction mode. To reduce errors caused by specimen drift and to avoid artifacts due to the lateral migration of Ca, the measurements were carried out using a broad beam in a piece of sample which is slightly smaller than the size of the SAD aperture. In this case the measured loss of species is solely due to sputtering from the surfaces. As shown in Fig. 6, both Ca and O drop almost immediately although the electron current density is lower than the threshold dose rate for the above mentioned damage (Fig. 1). The preferential sputtering of O is slightly easier than that of Ca. Most interestingly, it seems that the loss of Ca and O ceases at a certain point. We attribute this the

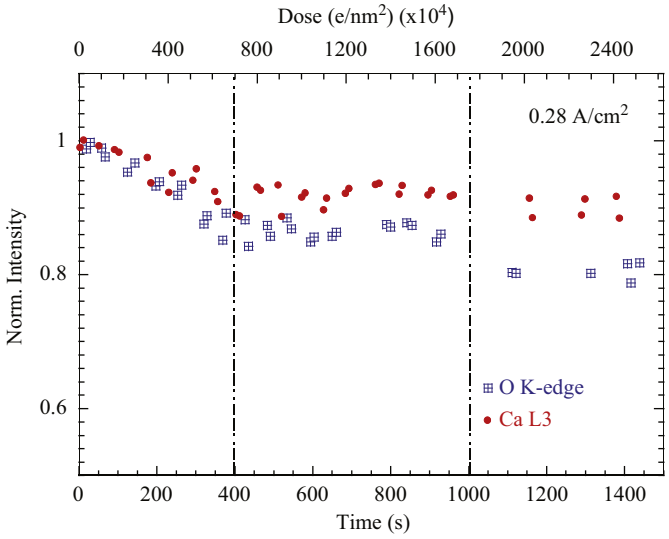

Fig. 6. Intensity profiles of Ca L_{23} and O K-edge EELS during beam damage.

phenomenon to the irradiation dependence of $E_s(t)$. The loss of species at different rates may reconfigure the surface structurally and compositionally and thus change the surface binding energies. Although it is reasonable to consider that surface sputtering is mainly due to knock-on interactions between energetic electrons and surface atoms, two other mechanisms (radiolysis and charging) may also affect the event. Similar to Electron-stimulated desorption (ESD), radiolysis may also result in the loss of O from the surface [32], and the electrostatic potential created by electron beam may also drive Ca out of sample.

Several common methods have been frequently considered to reduce or even prevent beam damage. One method is to cool the specimen down to liquid nitrogen or even liquid helium temperature. One should note that lowering the temperature may reduce the damage rate, but it may also reduce the recovery rate. Therefore, how effective this method needs serious investigation. One exception is the case of surface sputtering, in which the recovery rate is negligible anyway. It is reasonable to expect that lowering the temperature may reduce the sputtering rate.

Another commonly used method is to coat the surfaces of the specimen with amorphous C or another metal layer either to prevent sputtering or to increase the conductivity of specimen [33]. Perhaps this method can effectively prevent the preferential mass loss due to the sputtering, but it has not been tested seriously how effective it can be to reduce bulk damage, such as atom displacements and phase separation. Moreover, the C films may react with the specimen under electron beam irradiation. Therefore, adding extra matter to the sample may complicate the analysis. In our experiment, the glass sample was supported by the lacy C film. Fig. 7 compares the C K-edge EELS acquired at the beginning of irradiation with one recorded after long exposure. The C K-edge EELS is from a piece of C film supporting the glass sample. At the beginning of irradiation, the C K-edge shows a distinctive amorphous C features. However, after prolonged irradiation, the fine structure in the C K-edge changes significantly. The origin of the changes is unknown at this stage, but these changes are most likely caused by the reaction between C and damage products of the glass.

Therefore, an effective and practical way to apply electron microscopy techniques to beam sensitive materials remains to be found. If the threshold of dose rate observed in this study is a general phenomenon, lowering the dose rate (i.e. electron current density) can definitely avoid beam damage for a given total dose.

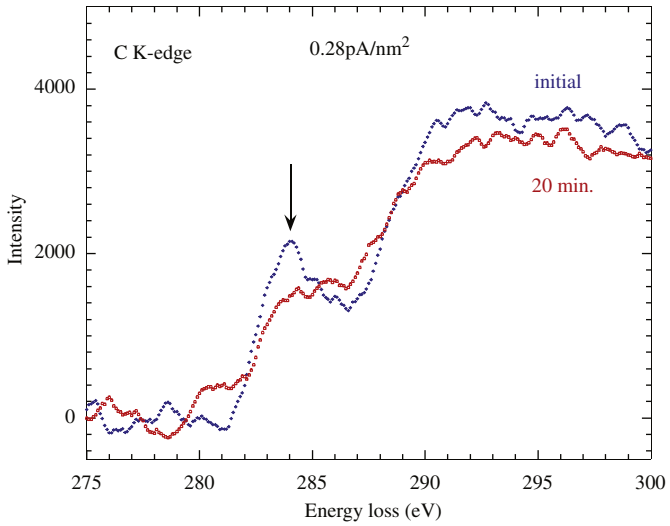

Fig. 7. Comparison of C K-edge before and after beam damage of sample.

Unfortunately, one has to compromise the high quality of SNR and spatial resolution. According to the discussion above, the time for excitation and ionization is much shorter than the time for an atomic displacement and recovery. Therefore, we can consider using electron pulses instead of "continuing" electron beam. Each electron pulse may contain hundreds to thousands of electrons, and the duration time for each pulse is in order of femtoseconds or sub-picoseconds, which is much shorter than the dwell time of current STEM. The interval of two consecutive pulses must be long enough for sample to recover from the damage induced by the previous electron pulse. Under this condition, one may expect to increase both the SNR and spatial resolution without worrying about beam damage. It should be pointed it out that this suggestion is based on the general existence of threshold dose rate to a specific type of damage. To increase the probability of recovery, the use of a higher temperature may be appropriate.

5. Conclusion

Electron beam damage in the CaF_2–Al_2O_3–SiO_2 glass has been studied using time dependent Ca L_{23} and O K-edge EELS. The damage involving formation of O defects depends on electron current density (dose rate). The damage cannot be detected at the dose rate lower than the threshold. The threshold phenomenon of dose rate may result from the competition of damage and recovery processes. The accumulation of damage can only occur when the damage rate is higher than the recovery rate. As one extreme case, the recovery rate for surface sputtering is negligible. Therefore, there is no threshold dose rate for surface sputtering.

Acknowledgment

This work is supported by DOE award DE-FG52-09NA29451. The CaF_2–Al_2O_3–SiO_2 glass was synthesized by Dr. S. Ye of Tongji University of China. The use of facilities within the Center for Solid State Science at ASU is also acknowledged.

References

[1] A.R. Lupini, O. Krivanek, N. Dellby, P.D. Nellist, S.J. Pennycook, Developments of Cs-corrected STEM, Institute of Physics Conference Series 168 (2001) 31–34.
[2] L.W. Hobbs, Murphy's law and the uncertainty of electron probes, Scanning Electron Microscopy Supplement 4 (1990) 171–183.
[3] R.F. Egerton, P. Li, M. Malac, Micron 35 (2004) 399.
[4] L.W. Hobbs, Ultramicroscopy 3 (1979) 381.
[5] L.W. Hobbs, M.R. Pascucci, Journal de Physique 41 (1980) 237 Colloque C6.
[6] J. Cazaux, Ultramicroscopy 60 (1995) 422.
[7] N. Jiang, J. Qiu, A. Garta, J. Silcox, Applied Physics Letters 80 (2002) 2005.
[8] N. Jiang, G. Humbree, J.C.H. Spence, J. Qiu, F.J.G. de Abajo, J. Silcox, Applied Physics Letters 83 (2003) 551.
[9] C.R. Bradley, Argonne National Laboratory Report No. ANL-88-48, (1988).
[10] P. Li, R.F. Egerton, Ultramicroscopy 101 (2004) 161.
[11] N. Jiang, J.C.H. Spence, Journal of Applied Physics 105 (2009) 123517.
[12] M. Isaacson, Inelastic scattering and beam damage in biological molecules, in: B.M. Siegel, D.R. Beaman (Eds.), Physical Aspects of Electron Microscopy and Microbeam Analysis, Wiley, New York, 1975 chapter 14.
[13] A. Howie, F.J. Rocca, U. Valdre, Philosophical Magazine B 52 (1985) 751.
[14] M.R. Stevens, Q. Chen, U. Weierstall, J.C.H. Spence, Transmission electron diffraction at 200 eV and damage threshold below the carbon K-edge, Microscopy and Microanalysis 6 (2000) 368–379.
[15] L. Reimer, Review of the radiation damage problem of organic specimens in electron microscopy, in: B.M. Siegel, D.R. Beaman (Eds.), Physical Aspects of Electron Microscopy and Microbeam analysis, Wiley, New York, 1975.
[16] R.F. Egerton, P.A. Crozier, P. Rice, Ultramicroscopy 23 (1987) 305.
[17] R.M. Glaeser, K. Downing, D. DeRosier, W. Chiu, J. Frank, Electron Crystallography of Biological Macromolecules, Oxford University Press, New York, New York, 2007, pp. 131–134.
[18] J.P. Buban, Q. Ramasse, B. Gipson, N.D. Browning, H. Stahlberg, Journal of Electron Microscopy 59 (2010) 103.
[19] L. Reimer, Transmission Electron Microscopy, 2nd edition, Springer, Berlin, 1989, pp. 431–463.
[20] F.R. Fryer, Ultramicroscopy 23 (1987) 321.
[21] I.G. Salisbury, R.S. Timsit, S.D. Berger, C.J. Humphreys, Applied Physics Letters 45 (1984) 1289.
[22] C.J. Humphreys, T.J. Bullough, R.W. Devenish, D.W. Maher, P.S. Turner, Scanning Electron Microscopy Supplement 4 (1990) 185–192.
[23] J.M. Macaulay, R.M. Allen, L.M. Brown, S.D. Berger, Microelectronic Engineering 9 (1989) 557.
[24] N. Jiang, Journal of Applied Physics 110 (2011) 013518.
[25] A.L. Ankudinov, B. Ravel, J.J. Rehr, S.D. Conradson, Physics Review B 58 (1998) 7565.
[26] N. Jiang, Solid State Communications 122 (2002) 7.
[27] N. Jiang, J. Qiu, A. Ellison, J. Silcox, Physics Review B 68 (2003) 064207.
[28] N. Jiang, J.C.H. Spence, Ultramicroscopy 106 (2006) 215.
[29] N. Jiang, Journal of Applied Physics 100 (2006) 013703.
[30] A.P. Hitchcook, C.E. Brion, Journal of Electron Spectroscopy and Related Phenomena 18 (1980) 1.
[31] J.F. DeNatale, D.G. Howitt, Radiation Effects 91 (1985) 89.
[32] M.R. McCartney, P.A. Crozier, J.K. Weiss, D.J. Smith, Vacuum 42 (1991) 301.
[33] R.F. Egerton, F. Wang, P.A. Crozier, Microscopy and Microanalysis 12 (2006) 65.